RSC Advances

ROYAL SOCIETY OF CHEMISTRY

www.rsc.org/advances

Graphical Abstract

Flexible all-solid-state supercapacitors based on graphene films with different gel electrolytes are demonstrated. During the bending and cycling of graphene-based solid-state supercapacitor, the stability could be maintained without sacrificing the electrochemical performance.

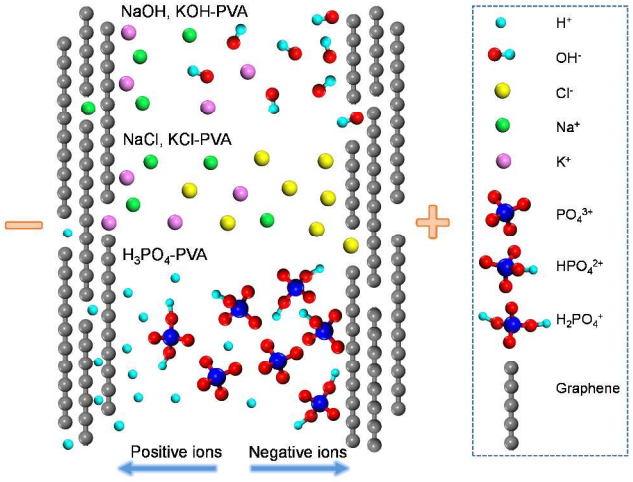

RSC Advances

RSCPublishing

ARTICLE

Effect of Different Gel Electrolytes on Graphene Based Solid-State Supercapacitors

Cite this: DOI:

Qiao Chen[a,b], Xinming Li[c], Xiaobei Zang[a], Yachang Cao[a], Yijia He[a,b], Peixu Li[d], Kunlin Wang[a], Jinquan Wei[a], Dehai Wu[d], Hongwei Zhu[a,b,*]

Received,
Accepted

DOI:

www.rsc.org/

A solid-state supercapacitor with flexible, simple structure is designed based on graphene thin film electrodes and acid/base/salt-PVA gel electrolytes. The performance of six different gel electrolytes (using H_3PO_4, H_2SO_4, KOH, NaOH, KCl, NaCl as electrically conductive substances) in this graphene based supercapacitor have been revealed. The electrochemical properties of the supercapacitor with high flexibility and stability is enhanced by optimizing the concentration of electrically conductive substance in polymer gel.

1. Introduction

Emergence of flexible and wearable electronic equipment proposes requirement of novel electronic components, *e.g.* bendable displays and power sources. Specifically, flexible supercapacitor, one of the most important energy storage devices has been extensively explored these years[1-4]. Based on various electrodes, different kinds of gel electrolytes with obvious advantages of solid-state and non-sealing for flexible supercapacitors have been developed[5,6]. Generally, gel electrolytes were prepared by admixing electrically conductive substance (acids, bases or salts to form conducting ions) with polymer (*e.g.* polyvinyl alcohol (PVA)) matrix in water and the frequently-used conductive substances were phosphoric, sulfuric acid and caustic potash.

As having a high specific surface area, high intrinsic carrier mobility and excellent mechanical properties[7,8] , graphene is a promising candidate for advanced electrode materials of supercapacitors[9]. The theoretical capacitance value calculated from single-layer graphene supercapacitor is as high as 550 F/g with all surface used[10,11]. A variety of graphene used in supercapacitors have been reported recently, such as punched disc electrodes[12], flexible flat thin film electrodes[11,13], microfiber electrodes for solid-state supercapacitors[14].

2. Experimental

In this work, we present a flexible, transparent solid-state supercapacitor based on graphene film electrodes and PVA gel electrolytes. Figure. 1a shows the fabrication process and structure illustration of the device. The few-layer graphene film grown by chemical vapor deposition (CVD) was cut into square with sides of 7~10 mm and was transferred directly onto the flexible substrate (polyethylene glycol terephthalate (PET)). Figure. 1b is a transmission electron microscope (TEM) image of the graphene film which was not only used as electrode but also as the current collector in this device. Then a thin layer of gel electrolyte was coated to the surface of the graphene electrode. Based on the scanning electron microscopy (SEM) observation (Figure. 1c: i), it is clearly seen that the PVA gel electrolyte has good contact with the graphene electrode. And there's hardly any transparency change of graphene electrode before and after coating electrolyte, where is separated by the white dashed in Figure 1c: ii. The as-assembled device contains two film electrodes, which are bound together by the gel electrolyte. The electrolyte also serves as separator and binding material. Furthermore, this supercapacitor is flexible and transparent as shown in Figure. 1d and the thickness of the device is mainly dependent on the polymer substrates.

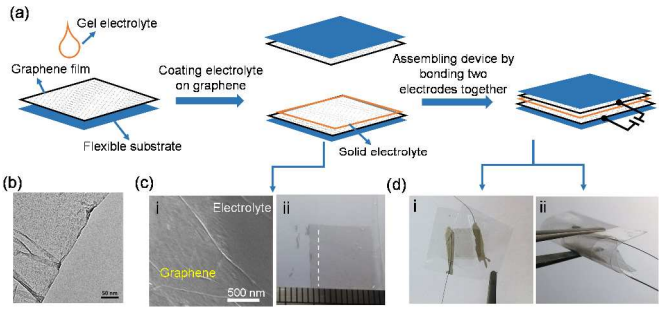

Figure 1. (a) Schematic illustration of the fabrication process of the solid-state supercapacitor. (b) TEM image of the graphene film. (c) Graphene film with part of coating electrolyte. i: SEM image; ii: digital photo, the white dashed separate graphene from coating gel electrolyte. (d) Photographs of the pristine (left) and bent (right) supercapacitors.

The electrochemical performances of as-prepared supercapacitors were evaluated using cyclic voltammetry (CV), galvanostatic charge/discharge and electrical impedance spectroscopy (EIS) in a two-electrode electrochemical cell system. The areal specific capacitance of the device was calculated from the CV curves by integrating the whole curve to gain an average value. The areal capacitance of supercapacitors was calculated by Eq. 1.

$$C = \int_{V_1}^{V_2} IdV / S\Delta V v \quad (1)$$

Where V_1 and V_2 represent the inception potential and terminal potential, respectively, $\int_{V_1}^{V_2} IdV$ is a half integral area of the CV curve, S is the surface area of the supercapacitor, $\Delta V = V_1 - V_2$ is the potential voltage window, and v is the potential scan rate. The voltage range of the gel electrolyte is similar to that of aqueous electrolyte (0.5~1 V)[15]. EIS was conducted at 0 V versus open circuit voltage from 100 kHz to 10 mHz and the data was analyzed by Nyquist plots which exhibit imaginary component (Z'') and real component (Z') of the impedance. At high frequencies (the lower left portion of the curve) there is an intersection of the plot on the real axis which represents the internal resistance of the supercapacitor. At the middle frequency region there is a 45° portion called Warburg region and is the respect for diffusion of the ions in the electrolyte[16,17].

3. Results and discussion

Kinds of different electrically conductive substances were used in PVA gel electrolyte. To figure out the most suitable gel electrolyte for the graphene based solid-state supercapacitors, six different electrolytes were used in this work, by mixing 0.01 mol conductive substance (H_3PO_4, H_2SO_4, KOH, NaOH, KCl, NaCl) and 1 g PVA in 10 mL deionized water following by stirring and heating. All the supercapacitors were tested in the condition where the gel electrolyte showed a stable performance. Figure. 2 shows the CV curves of the solid-state supercapacitors with different gel electrolytes at potential scan rate of 100 mV/s. As shown in Figure. 2a, the CV curve of H_3PO_4-PVA supercapacitor is near rectangular, which shows a typical characteristic of an ideal capacitor[18]. The specific capacitance calculated from the CV curve in a potential window from 0 to 0.8 V for H_3PO_4-PVA supercapacitor is 15 μF/cm^2, which is comparable to the measured double-layer capacitance of single-layer to bilayer graphene in ionic liquid electrolyte[10]. For H_2SO_4-PVA supercapacitor, as seen in Figure. 2b, there are two obvious redox peaks around ±0.25 V in the CV curve, corresponding to a specific capacitance of 820 μF/cm^2. H_2SO_4 might promote some certain redox reactions[19] in H_2SO_4-PVA electrolyte supercapacitor during charging and discharging. This H_2SO_4-PVA supercapacitor shows a several ten times higher capacitance value than H_3PO_4-PVA supercapacitor, however, as correlating with pseudo capacitance, the stability of H_2SO_4-PVA supercapacitor is poorer than other electrolytes used in this work. So the next work leave H_2SO_4-PVA electrolyte out of account for gaining more stable electrochemical performance. The CV curves of KOH-PVA and NaOH-PVA supercapacitors display high symmetrical and rectangular shapes (Figure. 2c), indicating good capacitance characteristics. However, in CV curves of KOH-PVA and NaOH-PVA supercapacitors, the current densities are low and the voltage window is narrow compared to H_3PO_4-PVA supercapacitor. The supercapacitors using neutral gel electrolytes (NaCl-PVA, KCl-PVA) show fusiform shaped CV curves (Figure. 2d) with about ten times lower specific capacitances comparing with H_3PO_4-PVA supercapacitors.

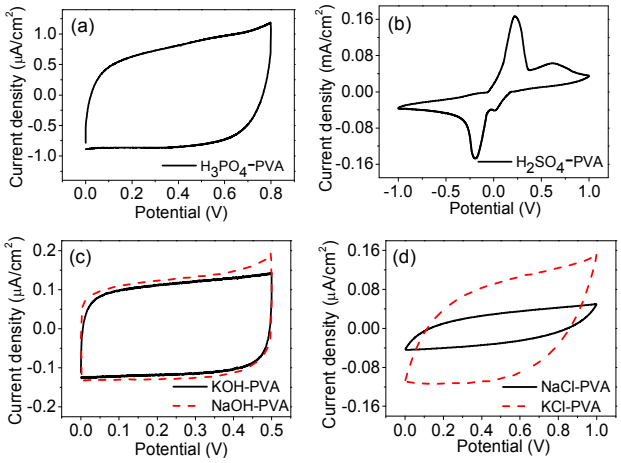

Figure 2. CV curves of as-prepared solid-state supercapacitors with different electrolytes at 100 mV/s scan rate. (a) H_3PO_4-PVA electrolyte. (b) H_2SO_4-PVA electrolyte. (c) Base gel electrolytes: KOH (black) and NaOH (red dashed), (d) Neutral gel electrolytes: NaCl (black) and KCl (red dashed).

The specific capacitance, power and energy density values of devices with six different gel electrolytes calculated from CV curves are shown in Table S1. Figure S1 shows the Ragone plots for the devices with those acid, base and salt electrolytes. For the supercapacitor using H_3PO_4-PVA gel electrolyte, both the energy and power density values are almost one order of magnitude higher than that of other four base and salt electrolytes. The results apparently show that for this graphene based supercapacitor, H_2SO_4-PVA gel electrolyte substantially increases the capacitance value with low cycle stability, while base electrolytes present good double layer electrochemical behaviour but with relatively lower capacitance, and the salt electrolytes show no obvious advantages than others. In a word, the H_3PO_4-PVA gel electrolyte shows the best overall electrochemical performance compared to others in the solid-state supercapacitor.

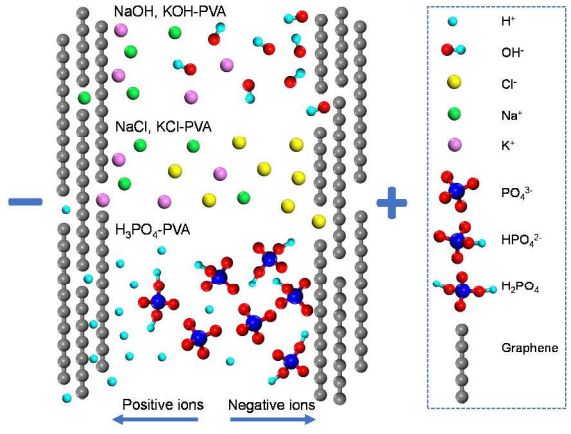

Figure 3. Schematic illustration of ions diffusion in different electrolytes.

Further comprehension about the effect of different electrolytes on the supercapacitors has achieved with

theoretical analysis. As shown in Figure. 3, the few-layer graphene film is comprised of many graphene sheets. The ionic radius of H^+ in H_3PO_4-PVA electrolyte is extremely smaller than that of the ions (Na^+, K^+, OH^-, Cl^-)[20] ionized from the base or salt in the gel electrolyte. The H^+ ions could easily and quickly diffuse in between the graphene layers. While the heavy ions, such as Na^+ or K^+ with large size could only reach the surface of graphene electrode during charging and discharging. Meanwhile, H_3PO_4 could ionize more free ions than NaOH or NaCl at the same molar concentration. For electrolytes with low ion concentration, the capacitance of the supercapacitor increase with the ion concentration in electrolyte[21,22]. Thus, the supercapacitor using H_3PO_4-PVA gel electrolyte shows higher specific capacitance than base/salt electrolyte.

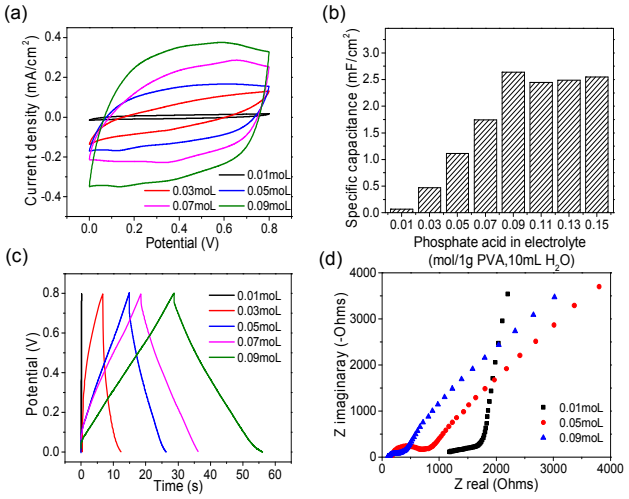

Figure 4. Electrochemical properties of solid-state supercapacitors with different concentrations of H_3PO_4-PVA electrolytes. (a) Cyclic voltammetry curves at 100 mV/s. (b) Areal specific capacitances at 100 mV/s (H_3PO_4: 0.01~0.15 mol). (c) Galvanostatic charge/discharge curves at 0.1 mA/cm^2. (d) Nyquist impedance plots of the devices using 0.01, 0.05 and 0.09 mol H_3PO_4 electrolyte.

To understand the relationship between the electrolyte concentrations with its electrochemical performance to further obtain better results, an optimization of H_3PO_4-PVA electrolyte was conducted then. As shown in Figure. 4, the electrochemical properties of graphene-based solid-state supercapacitors vary along with the concentration (0.01~0.15 mol) of H_3PO_4 in gel electrolytes. The current density increases gradually with the H_3PO_4 loading and the CV curves remain nearly rectangular (Figure. 4a) and the galvanostatic charge/discharge test in Figure. 4c shows the same trend. Corresponding area specific capacitance values calculated from CV test are shown in Figure. 4b. It seems that the capacitance properties increases at the concentration range of 0.01~0.09 mol and becomes steady with further increasing from 0.09 to 0.15 mol. In Figure. 4d, Nyquist plots of three typical graphene-based solid-state supercapacitors with 0.01, 0.05 and 0.09 mol H_3PO_4-PVA are compared. The plot of the device with 0.09 mol electrolyte exhibits a lower internal resistance and a smaller semicircular diameter at high frequency to Warburg region, indicating a better interface nature between electrolyte and electrode. The results confirm the assumption that high ions concentration in gel electrolytes cloud advance capacitance performance within certain range and are also in good agreement with previous reports[21,22].

Overall, an optimized high specific capacitance of about 2.6~3.7 mF/cm^2 was achieved in the device with 0.09 mol H_3PO_4-PVA gel electrolyte. The performance is superior compared to planar graphene and reduced graphene oxide based supercapacitors (80-394 μF/cm^2)[15], electrochemical micro-supercapacitors (0.4~2 mF/cm^2)[14,23,24], and laser-scribed graphene supercapacitor in organic electrolyte (2.07~4.82 μF/cm^2)[11]. The power density of the 0.09 mol H_3PO_4-PVA supercapacitor could reach 0.106 mW/cm^2 and the energy density was measured to be 0.235μWh/cm^2. The electrochemical performance of the solid-state supercapacitor with optimized H_3PO_4-PVA electrolyte is displayed in Figure. 5. CV scans of the device show nearly rectangular shapes at different scan rates (10~200 mV/s) (Figure. 5a), indicating an efficient capacitive behaviour, which results from adequate ions concentration in electrolyte and high electrochemical capability of graphene electrode, enabling fast ions transportation. As seen in Figure. 5b, the galvanostatic charge/discharge curves of the device at various current densities (0.05~0.5 mA/cm^2) are close to triangular shapes, revealing an ideal capacitive performance and a balance charge across electrodes[25,26]. Moreover, graphene-based solid-state supercapacitors demonstrate high flexibility (Figure. 5c) during bending to 180°, which means good contact between graphene electrodes and PVA electrolyte[2]. As shown in Figure. 5d, the as-assembled supercapacitor shows good stability over 5000 cycles with no performance degradation.

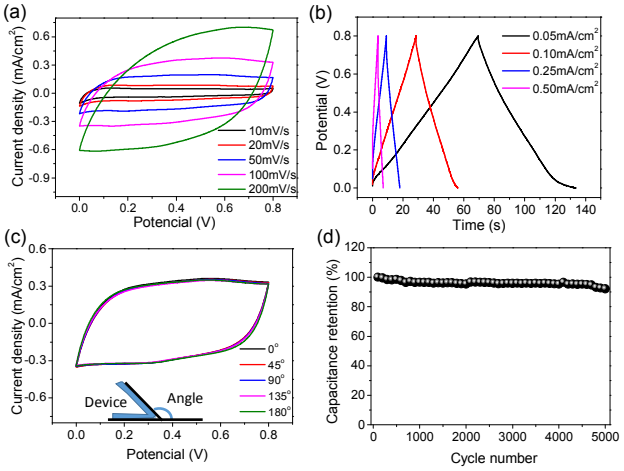

Figure 5. Electrochemical performance characterizations of solid-state supercapacitors with optimized H_3PO_4-PVA electrolyte. (a) CV curves at different scan rates, (b) Galvanostatic charge/discharge curves at different current densities, (c) CV curves collected at 100 mV/s for the device with different bending angles and the inset is the schematic illustration of the bent device, (d) Cyclic stability tested at 100 mV/s over 5000 cycles.

4. Conclusion

To conclude, by comparing the electrochemical performance of the as-assemble bendable supercapacitors with different acid/base/salt-PVA gels electrolytes, H_3PO_4-PVA electrolyte stands out as operating better with graphene electrode. The effect of the concentration of H_3PO_4 in gel electrolyte on the electrochemical performance of the solid state supercapacitors has been studied. The optimized PVA gel electrolyte could be

extended to other graphene-based supercapacitors to raise the capacitance properties.

Notes and references

[a] School of Materials Science and Engineering, State Key Laboratory of New Ceramics and Fine Processing, Tsinghua University, Beijing 100084, China.
[b] Center for Nano and Micro Mechanics, Tsinghua University, Beijing 100084, China.
[c] National Center for Nanoscience and Technology, Zhongguancun, Beijing 100190, China.
[d] Department of Mechanical Engineering, Tsinghua University, Beijing 100084, China.
*Email: hongweizhu@tsinghua.edu.cn.

Electronic Supplementary Information (ESI) available: Performance summary and Ragone plots of the devices. See DOI: xxx.

Acknowledgements

This work was supported by the Beijing Natural Science Foundation (2122027).

1 X. M. Li, T. S. Zhao, Q. Chen, P. X. Li, K. L. Wang, M. L. Zhong, J. Q. Wei, D. H. Wu, B. Q. Wei and H. W. Zhu, Phys. Chem. Chem. Phys., 2013, **15**, 17752.
2 X. B. Zang, Q. Chen, P. X. Li, Y. J. He, X. Li, M. Zhu, X. M. Li, K. L. Wang, M. L. Zhong, D. H. Wu and H. W. Zhu, *Small*, 2014, **10**, 2583.
3 C. Z. Meng, C. H. Liu, L. Z. Chen, C. H. Hu and S. S. Fan, Nano Lett., 2010, 10, 4025.
4 G. P. Xiong, C. Z. Meng, R. G. Reifenberger, P. P. Irazoqui and T. S. Fisher, Adv. Energy Mater., 2014, **4**, 1300515.
5 J. Bae, M. K. Song, Y. J. Park, J. M. Kim, M. L. Liu and Z. L. Wang, *Angew. Chem. Int. Edit*., 2011, **50**, 1683.
6 V. K. Thakur, G. Q. Ding, J. Ma, P. S. Lee and X. H. Lu, *Adv. Mater.*, 2012, **24**, 4071.
7 A. K. Geim and K. S. Novoselov, *Nat. Mater.*, 2007, **6**, 183.
8 J. C. Meyer, A. K. Geim, M. I. Katsnelson, K. S. Novoselov, T. J. Booth and S. Roth, *Nat.*, 2007, **446**, 60.
9 C. H. Xu, B. H. Xu, Y. Gu, Z. G. Xiong, J. Sun and X. S. Zhao, *Energy. Environ. Sci.*, 2013, **6**, 1388.
10 J. L. Xia, F. Chen, J. H. Li and N. J. Tao, *Nat. Nanotechnol.*, 2009, **4**, 505.
11 M. F. El-Kady, V. Strong, S. Dubin and R. B. Kaner, *Sci.*, 2012, **335**, 1326.
12 M. D. Stoller, S. J. Park, Y. W. Zhu, J. H. An and R. S. Ruoff, *Nano. Lett.*, 2008, **8**, 3498.
13 H. P. Cong, X. C. Ren, P. Wang and S. H. Yu, *Energy. Environ. Sci.*, 2013, **6**, 1185.
14 Y. N. Meng, Y. Zhao, C. G. Hu, H. H. Cheng, Y. Hu, Z. P. Zhang, G. Q. Shi and L. T. Qu, *Adv. Mater.*, 2013, **25**, 2326.
15 J. J. Yoo, K. Balakrishnan, J. S. Huang, V. Meunier, B. G. Sumpter, A. Srivastava, M. Conway, A. L. M. Reddy, J. Yu, R. Vajtai and P. M. Ajayan, *Nano Lett.*, 2011, **11**, 1423.
16 P. L. Taberna, P. Simon and J. F. Fauvarque, *J. Electrochem. Soc.*, 2003, **150**, A292.
17 X. Yang, F. Zhang, L. Zhang, T. F. Zhang, Y. Huang and Y. S. Chen, *Adv. Funct. Mater.*, 2013, **23**, 3353.
18 E. Frackowiak and F. Beguin, *Carbon*, 2001, **39**, 937.
19 L. Staudenmaier and Ber. Dtsch, *Chem. Ges.*, 1898, **31**, 1481.
20 J. E. Huheey, E. A. Keiter and R. L. Keiter, in *Inorganic Chemistry : Principles of Structure and Reactivity*, HarperCollins, New York, 1993.
21 V. Srinivasan and J. W. Weidner, *J. Electrochem. Soc.*, 2000, **147**, 880.
22 J. P. Zheng and T. R. Jow, *J. Electrochem. Soc.*, 1997, **144**, 2417.
23 M. Kaempgen, C. K. Chan, J. Ma, Yi Cui and G. Gruner, *Nano Lett.*, 2009, **9**, 1872.
24 D. Pech, M. Brunet, H. Durou, P. H. Huang, V. Mochalin, Y. Gogotsi, P. L. Taberna and P. Simon, *Nat. nanotechnol.*, 2010, **5**, 651.
25 R. Kotz and M. Carlen, *Electrochem. Acta.*, 2000, **45**, 2483.
26 A. Burke, *J. Power Sources,* 2000,**91**, 37.

